MAGI-3 competes with NHERF-2 to negative regulate LPA_2 receptor signaling in colon cancer cells

Sei-Jung Lee, Stefanie L. Ritter, Huanchun Zhang, Hyunsuk Shim, Randy A. Hall, and C. Chris Yun

Supplementary Materials and Methods

Antibodies:

The generation of rabbit anti-NHERF-2 polyclonal antibody and mouse anti-VSVG monoclonal antibody was described previously [1]. Rabbit anti-V5 polyclonal was purchase from Covance (Princeton, NJ), and mouse anti- MAGI-3 monoclonal and mouse anti- $G\alpha_q$ monoclonal antibodies were from BD Biosciences (San Diego, CA). Mouse anti-Flag monoclonal was obtained from Sigma (St. Louis, MO). Rabbit anti-PLC-β3 polyclonal, rabbit anti-$G\alpha_{12}$ polyclonal, rabbit anti-$G\alpha_i$ polyclonal, mouse anti-IκBα monoclonal, rabbit anti-phospho-IκBα monoclonal, rabbit anti-NF-κBp65 polyclonal, mouse anti-β-actin monoclonal, mouse anti-phospho-JNK monoclonal, rabbit anti-JNK monoclonal, rabbit anti-phospho-c-Jun polyclonal, and rabbit anti-c-Jun monoclonal antibodies were obtained from Cell Signaling (Danvers, MA).

Inositol phosphates (IP) generation:

Cells were labeled with 1 μCi of myo-[^{3}H]-inositol (PerkinElmer, Waltham, MA) in 2 mL of serum-free medium for 24 h as previously described[2]. Labeled cells were treated with 20 mM LiCl for 15 min, followed by treatment with 1μM LPA for 20 min. Cells were resuspendend in 1.2 mL H_2O and extracted in 1.8 mL chloroform/methanol (1:2, v/v), and the upper phase was applied to a Dowex AG 1-X8 anion exchange column (Bio-Rad). The column was washed with 4 mL H_2O and then with 10 mL of 60 mM ammonium formate/5 mM sodium tetraborate. The accumulated myo-[^{3}H]-inositol

phosphates were eluted with 2 mL of 1 M ammonium formate/0.1 M formic acid. Radioactivity was measured with a β-scintillation counter.

Western immunoblot and immunoprecipitation: Western blotting and immunoprecipitation was performed as previously described [10]. To investigate the interaction between MAGI-3 and PLC-β isotypes, HCT116 cells were co-transfected using Lipofectamine 2000 (Invitrogen, Carlsbad, CA) with pcDNA3.1/V5-His-MAGI-3 and Flag-PLCβ isotypes. The monoclonal anti-V5, monoclonal anti-MAGI-3, and polyclonal anti-Oct-1 antibodies were from Covance, BD Biosciences, Abcam (Cambridge, MA), respectively. Isolation of cytoplasmic proteins for the detection of IκBα and nuclear proteins for the detection of NF-κBp65 were done using NE-PER Nuclear and Cytoplasmic Extraction Reagents Kit (Pierce, Rockford, IL). Co-immunoprecipitation of LPA_2, MAGI-3, NHERF-2, and PLC-β3 was performed using the Catch and Release System (Millipore, Billerica, MA) according to the manufacturer's instructions.

Cell Surface Expression Assay: The expression level of LPA_2 on the plasma membrane was quantified as described [13]. HCT116 cells stably expressing VSVG-LPA_2 were transfected with either MAGI-3 siRNA or NHERF-2 siRNA. The cells were washed with PBS, fixed in 4% paraformaldehyde, and blocked in PBS containing 2% nonfat dry milk for at least 30 min. Cells were incubated with an anti-VSVG antibody for 2 h at room temperature and treated with horseradish peroxidase-conjugated secondary antibody for 1 h. After three 15 min washes with PBS, cells were incubated with SuperSignal ELISA ECL reagent for 15 s. The luminescence, which corresponds to the amount of LPA_2 on the cell surface, was determined by using a TD 20/20 luminometer (Turner Designs, Sunnyvale, CA).

Immunohistochemical analysis of colon tissue array:

Human colon tissue array slides (IMH-359) were purchased from Imgenex. Immunohistochemical labeling was performed as previously described [3], except that

after the incubation with biotinylated secondary antibody solution the slides were incubated for 6 min with a diaminobenzidine tetrahydrochlorine substrate (DAB+, Dako), counterstained with hematoxylin, and dehydrated. The expression levels of MAGI-3 and NHERF-2 in tissue microarrays were quantified according to the published methods[4, 5]. Histological scoring of MAGI-3 and NHERF-2 expression was performed independently by two co-authors. Briefly, the intensity of cytoplasmic and plasma membrane immunostaining was subjectively scored on a scale of 0 (no staining) to 3 (strongest intensity), and the percentage of cells positively stained at the cytoplasm or plasma membrane was estimated at each intensity. The percentage of cells (from 0 to 100) was multiplied by the corresponding immunostaining intensity (from 0 to 3) to obtain histological scores ranging from 0 to 300. All tissue microarray experiments were repeated 3 times and the replicated results of each author were averaged.

References for Supplementary

1. Yun, CH, Lamprecht, G, Forster, DV, et al. NHE3 kinase A regulatory protein E3KARP binds the epithelial brush border Na^+/H^+ exchanger NHE3 and the cytoskeletal protein ezrin. J Biol Chem 1998;273:25856-25863.
2. Berridge, MJ, Downes, CP, Hanley, MR. Lithium amplifies agonist-dependent phosphatidylinositol responses in brain and salivary glands. Biochem J 1982;206:587-595.
3. Lin, S, Wang, D, Iyer, S, et al. The absence of LPA2 attenuates tumor formation in an experimental model of colitis-associated cancer. Gastroenterology 2009;136:1711-1720.
4. Buck, E, Eyzaguirre, A, Barr, S, et al. Loss of homotypic cell adhesion by epithelial-mesenchymal transition or mutation limits sensitivity to epidermal growth factor receptor inhibition. Mol Cancer Ther 2007;6:532-541.
5. Wang, Q, Sun, Z, Yang, HS. Downregulation of tumor suppressor Pdcd4 promotes invasion and activates both β-catenin/Tcf and AP-1-dependent transcription in colon carcinoma cells. Oncogene 2008;27:1527-1535.
6. Lin, S, Lee, SJ, Shim, H, et al. The Absence of LPA receptor 2 Reduces the Tumorigenesis by Apc^{Min} Mutation in the Intestine. Am J Physiol Gastrointest Liver Physiol 2010. in press.

SUPPLEMENTARY FIGURE LEGENDS

Supplementary Figure S1: MAGI-3 negatively regulates cell migration and invasion of HCT116 cells.

(**A**) HCT116 cells stably transfected with pLPCX or pLPCX/LPA_2 were seeded and serum-starved for 24 h. Cell-free regions were created by scraping with a pipet tip. Cells were then incubated in serum-free media supplemented with 1 μM or 10 μM of LPA. Migration of cells into cell-free areas was visualized. Cell migration of **(B)** HCT116/LPA_2 siRNA, (**C**) HCT116/NHERF-2 and HCT116/MAGI-3, and **(D)** HCT116/NHERF-2 siRNA and HCT116/MAGI-3 siRNA was determined. Representative figures from 3 independent experiments are shown. Data are represented as the means ± S.E. Scale bars; 200 μm **(E)** Invasive capacity of HCT116/pcDNA, HCT116/NHERF-2 and HCT116/MAGI-3 cells was assessed in BioCoat Matrigel Invasion Chambers with 8.0 μm pore membranes. Cells were removed from the upper chamber with a cotton swab and the cells that invaded the lower surface of the membrane were stained with H&E. Representative figures from 3 independent experiments are shown. Data are represented as the means ± S.E. Scale bars; 20 μm. **(F)** Cell invasion of SW480 cells transfected with pcDNA or pcDNA/MAGI-3 was determined.

Supplementary Figure S2: LPA-induced invasion of colon cancer cells is dependent on PLC activity.

LPA-induced invasion of HCT116 cells was determined in the presence or absence of the PLC inhibitor U73122 (5 μM). LPA-induced migration of HCT116 cells was abrogated in the presence of the PLC inhibitor U73122, suggesting that LPA-induced cell invasion is PLC-dependent. Scale bars; 20 μm. Quantification of cell invasion is shown on the right. n = 3.

Supplementary Figure S3: MAGI-3 inhibits PLC activation induced by ATP.

HCT116 cells transfected with **(A)** pcDNA or pcDNA-MAGI-3, or **(B)** control or MAGI-3 siRNA were treated with 10 μM ATP and the amounts of IPs generated were determined. The PLC activity was measured as described earlier. n = 3.

Supplementary Figure S4: MAGI-3 and NHERF-2 do not alter the amount of total Gα protein mediated by LPA_2.

(A) LPA-induced binding of [^{35}S]GTPγ-S in HCT116 cells transfected with control vector pLPCX or pLPCX/VSVG-LPA_2 was determined as described in Methods. n = 4. **(B)** The effects of NHERF-2 or MAGI-3 overexpression on the binding of [^{35}S]GTP-γ-S induced by LPA were determined.

Supplementary Figure S5: The effects of inhibitors on LPA-induced activation of NF-κB and JNK.

(**A**) HCT116 cells were pretreated with NBD peptide (10 μM) for 12 h, SP600125 (5 μM) for 3 h, or Gö6976 (1 μM) for 30 min prior to LPA treatment for 24 h. Cell invasion was detected by a Matrigel invasion assay as described in Methods. The panel on the right shows quantification of cell invasion. n = 3. (**B**) HCT116 cells were treated with LPA in the presence of SP600125 or U73122. Phosphorylation of IκBα was determined by Western blotting. (**C**) Cells were treated with LPA in the presence of U73122 or NBD, and phosphorylation of JNK was determined. n = 3 for each experimental set. (**D**) The effect of the PKC inhibitor Gö6976 on phosphorylation of c-Jun was determined. n = 3 for each experimental set.

Supplementary Figure S6: The phosphorylation level of IκBα is reduced in mouse tumors in the absence of LPA_2

The phosphorylation level of IκBα was determined in mouse intestinal tumors. The mouse intestinal lysates were from our published studies [3, 6]. (A) Equal amounts of lysates prepared from intestinal epithelial cells of WT or LPA_2-deficient (*Lpar2*$^{-/-}$) and adenomas of *Apc*$^{Min/+}$ or *Apc*$^{Min/+}$/*Lpar2*$^{-/-}$ mice were analyzed for phosphorylation levels of IκBα. The expression levels of total IκBα from each sample are shown in the bottom panel. (B) The expression levels of phosphorylated and total IκBα in intestinal lysates of WT and *Lpar2*$^{-/-}$ treated with azoxymethane (AOM) and dextran sodium sulfate (DSS) or not are shown. Representative results from 3 independent experiments are shown.

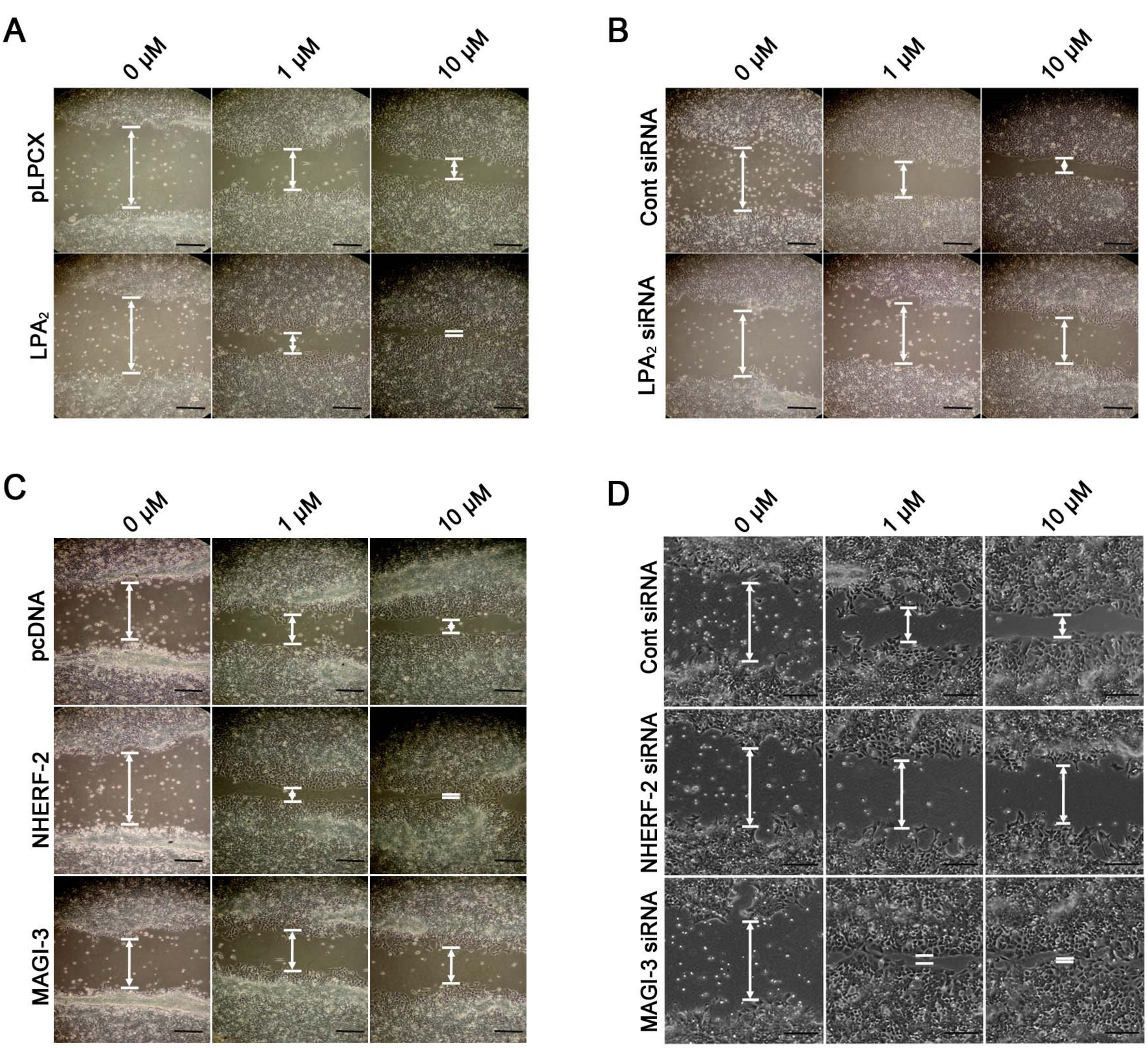

Supplementary Figure S1

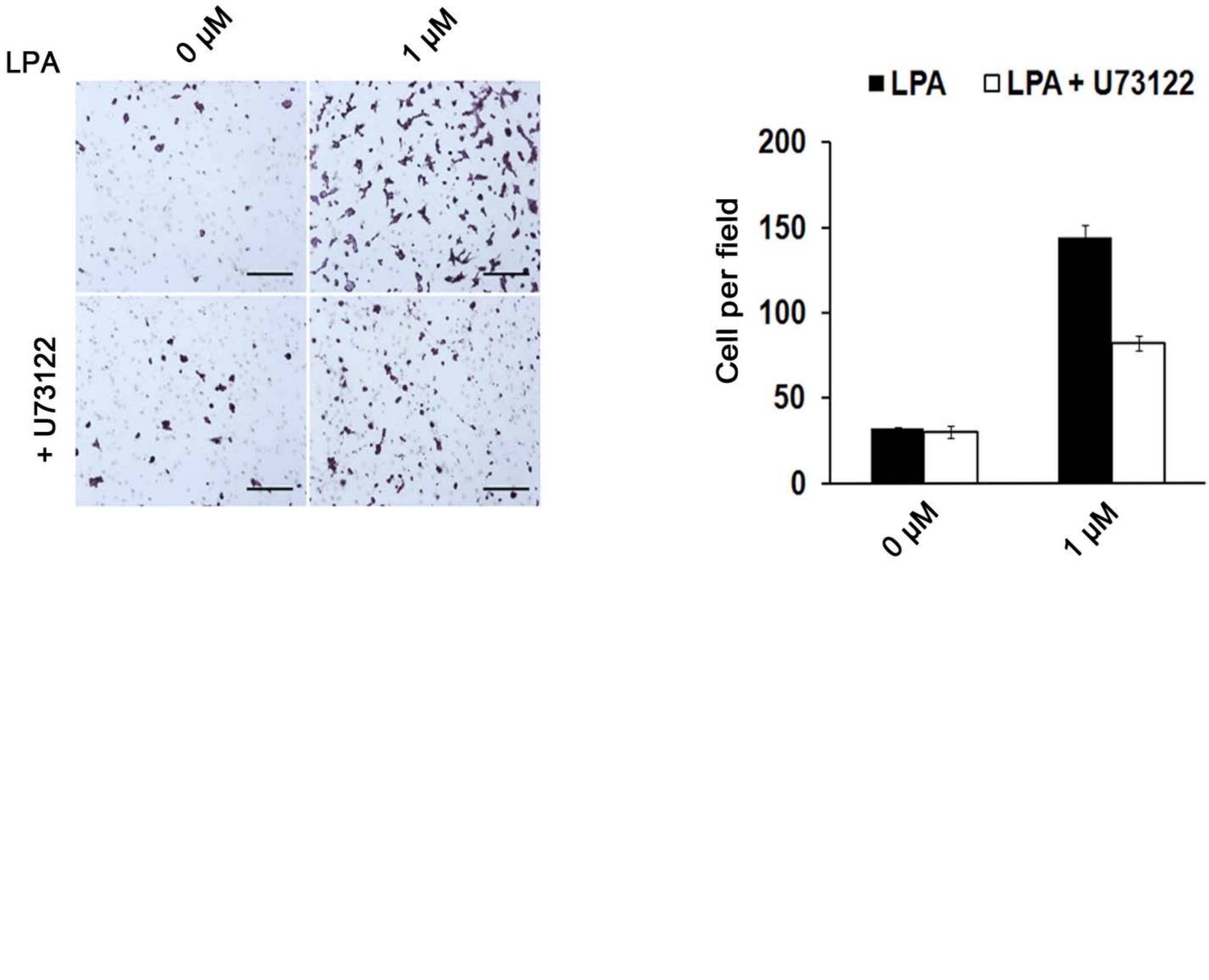

Supplementary Figure S2

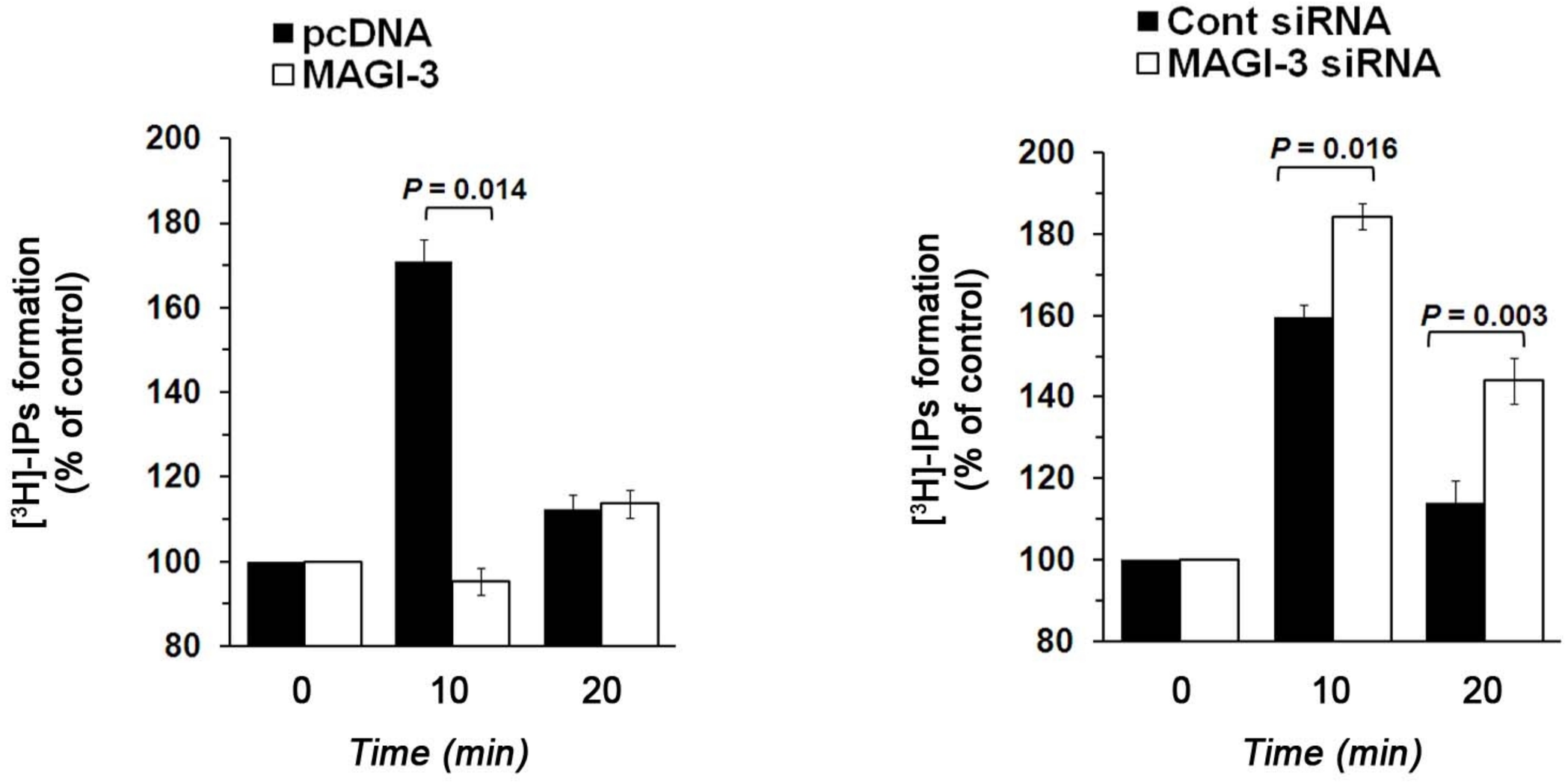

Supplementary Figure S3

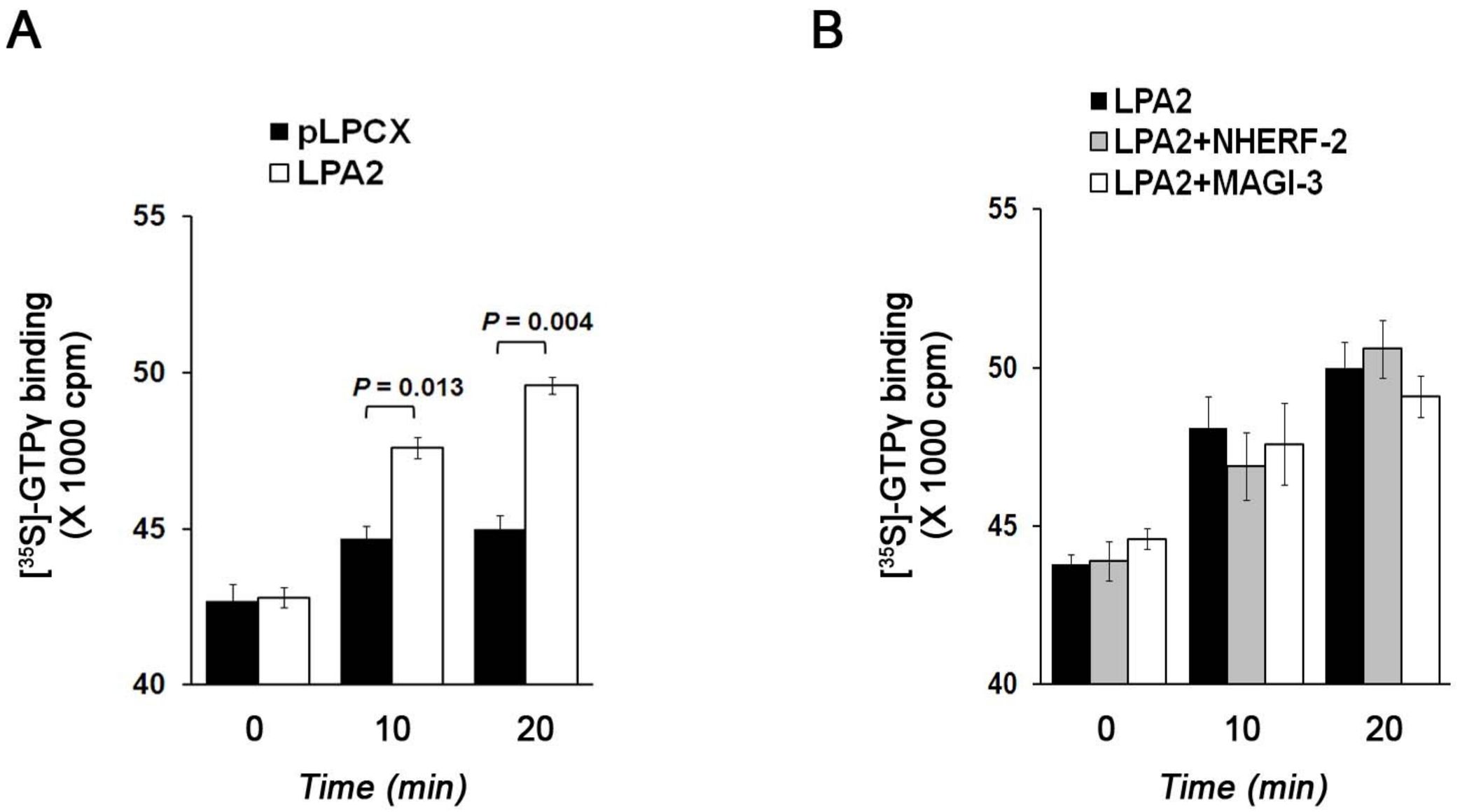

Supplementary Figure S4

A

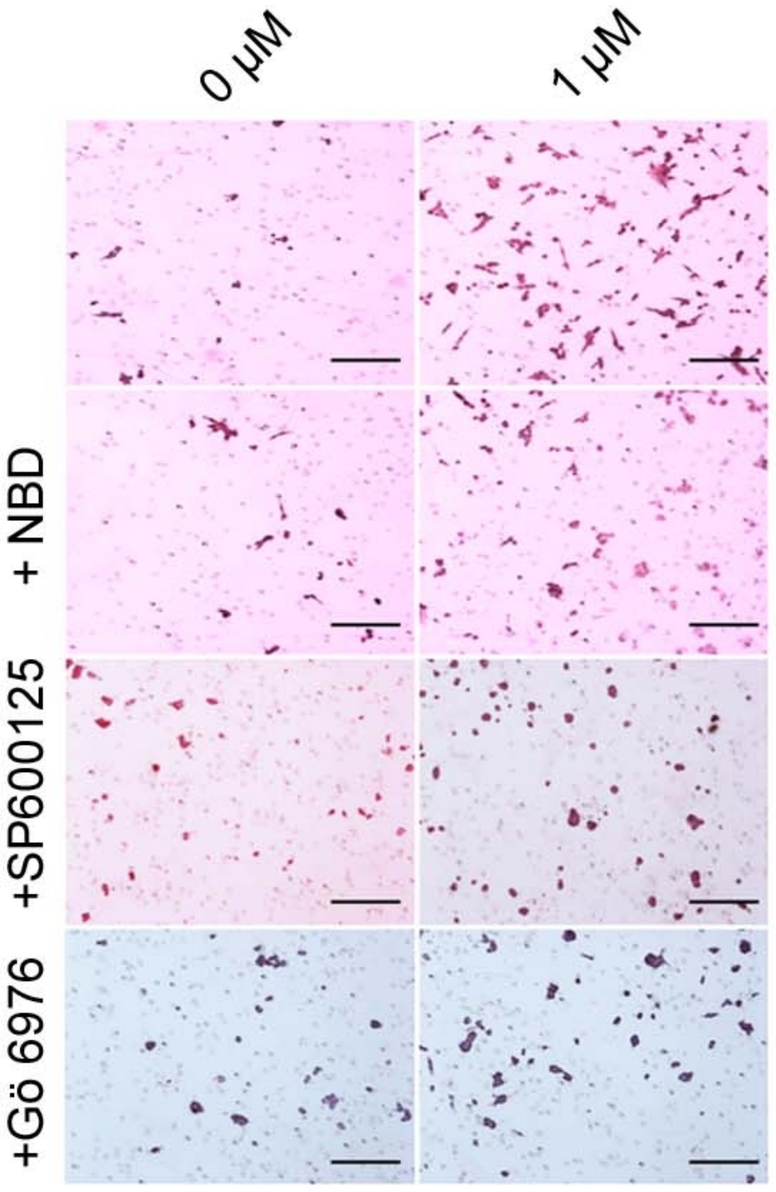

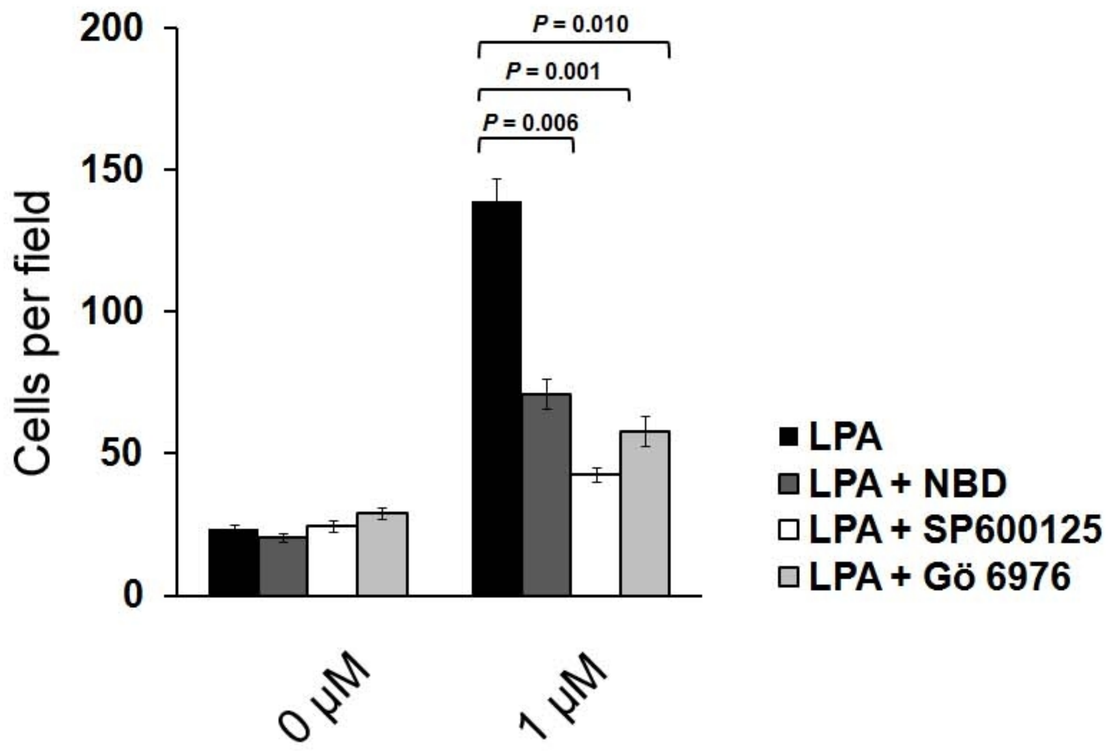

B

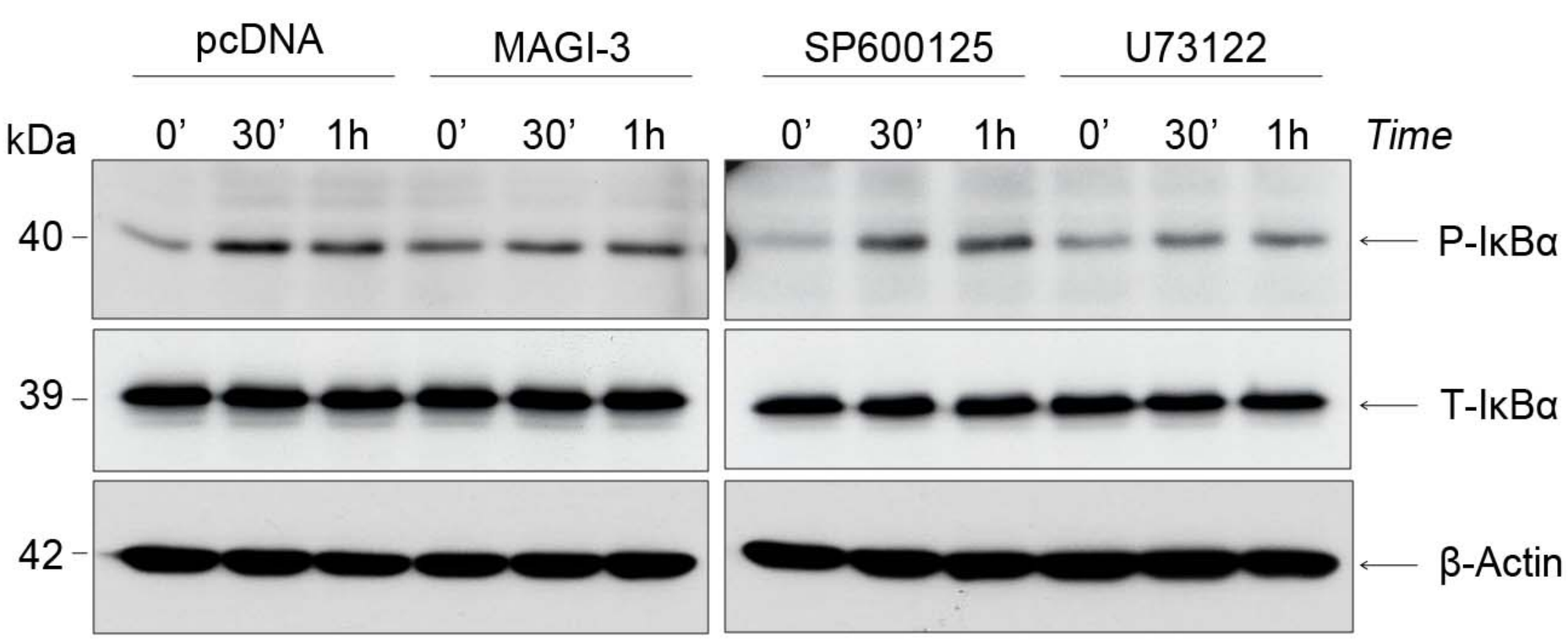

C

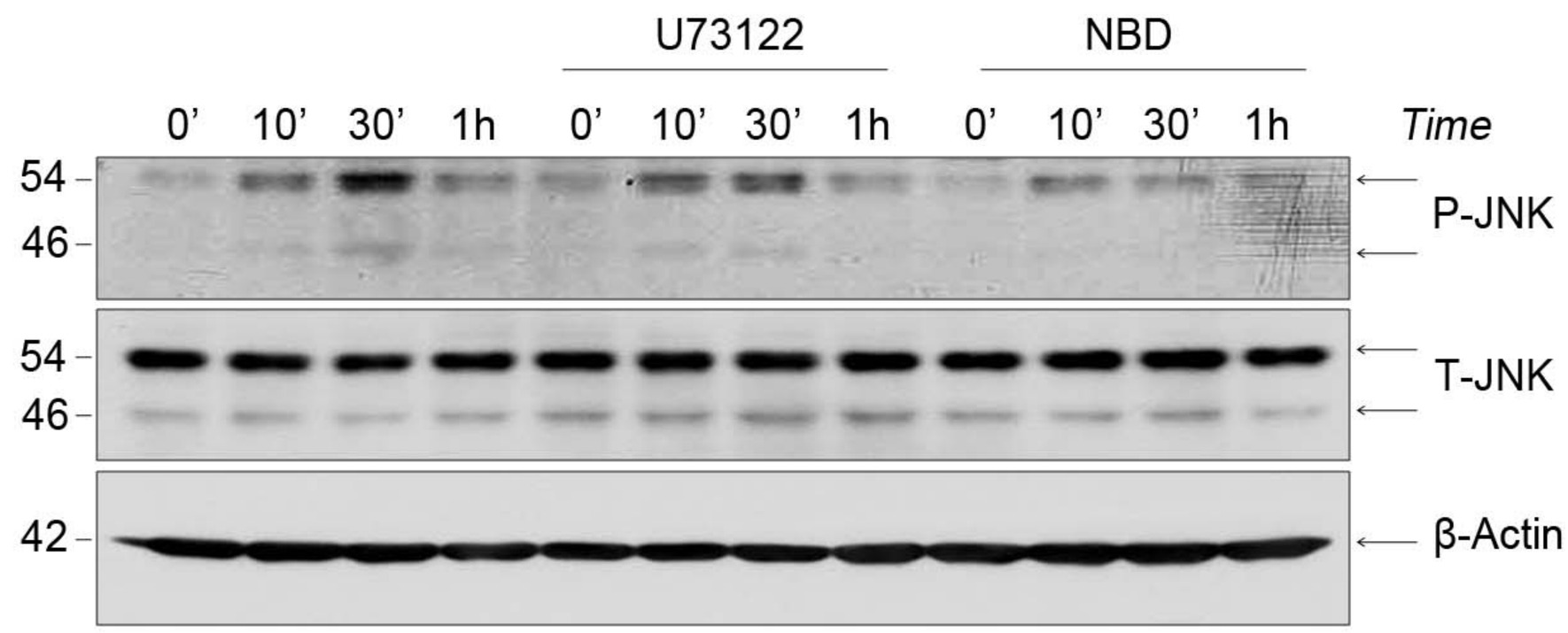

D

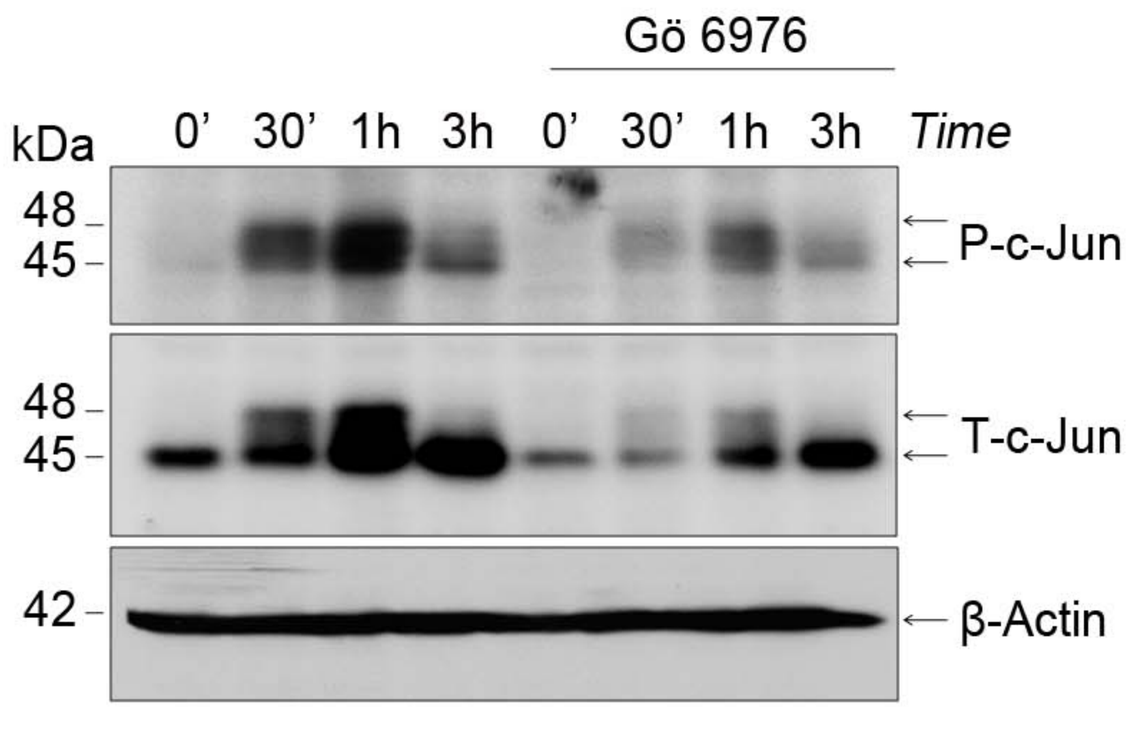

Supplementary Figure S5

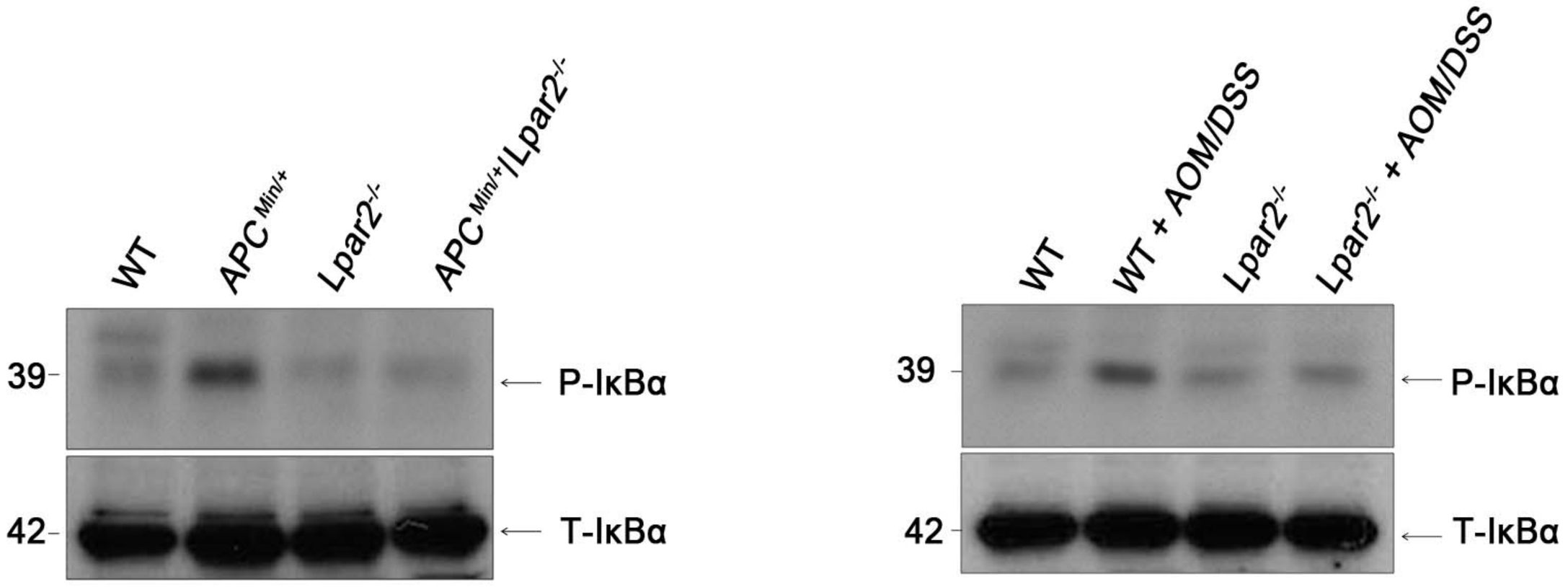

Supplementary Figure S6